Structural inhomogeneity in Silicon-On-Insulator probed with Coherent X-ray Diffraction

Xiaowen Shi[a*], Gang Xiong[a], Xiaojing Huang[a,b], Ross Harder[b] and Ian Robinson[a,c]

[a]London Centre for Nanotechnology and Department of Physics and Astronomy, University College London, WC1E 6BT U.K.

[b]Advanced Photon Source, Argonne National Laboratory, 9700 S. Cass Avenue
Argonne, IL 60439 U.S.A.

[c]Diamond Light Source, Harwell Campus, , OX11 0DE U.K.

Received ; Accepted

Keywords: Coherent, Inhomogeneity, X-ray Diffractive Imaging, Silicon-On-Insulator

Abstract

We report our research on X-ray micro-beam diffraction and Coherent X-ray diffractive imaging techniques to study structural inhomogeneities in Silicon-On-Insulator continuous plain wafers. Inhomogeneities were measured quantitatively and attributed to limitations of the manufacturing process. 3-dimensional image reconstructions were performed by using our Error-Reduction and Hybrid-Input-Output iterative algorithms. These revealed images of the focussed X-ray beam passing through the active layer of the wafer.

1 Introduction to Silicon-On-Insulator (SOI) Technology

1.1 SOI technology overview

Silicon-On-Insulator (SOI) technology has been widely recognized as a major industrial breakthrough during the past decade, offering significant improvements of metal–oxide–semiconductor field-effect transistor (MOSFET) device performance in terms of lower power dissipation, higher switching frequency and lower parasitic capacitance. SOI based MOSFETs are considered to be one of the best alternatives to conventional bulk-Silicon MOSFET technology, however, fabrication of SOI wafers are significantly more technologically challenging as the dimensions of the devices shrink dramatically. State-of-Art lithography-based fabrication techniques[1] are starting to be employed to overcome the possibility of strain arising from SOI fabrication[2].

1.2 SOI fabrication techniques

Various methods are used to fabricate Silicon-On-Insulator wafers: hetro-epitaxy, Separation by Implantation of Oxygen (SIMOX) [3][4] and Smart Cut™ technology[5] [6]. The SIMOX technique is particularly widely used due to relatively low crystal-defect density, low variation of film thickness and high crystalline-quality leading to high-quality wafers with high charge-carrier mobility. The SIMOX process involves Oxygen ion implantation onto single-crystalline Silicon wafer, during which oxidation occurs; a subsequent high-temperature annealing process recovers the high-quality crystalline structure of film. Smart

* Correspondence author (xiaowen.shi.09@ucl.ac.uk)

Cut™ technology involves transferring high-quality single crystalline Silicon thin layer from wafer to wafer, and is followed by annealing and final polishing processes.

In the experiments reported here, we used a Silicon (111) substrate ("handle") to have a different crystallographic orientation from that of the top Silicon layer (001) studied. This allowed the diffraction signal from the active top Silicon layer to be independent of interference from the substrate. SIMOX material is unsuitable for the experiments because the signal from the thin film would always be swamped by that of the substrate. The wafer we measured was specially ordered from Siegert Consulting Company, Germany, and manufactured by the film transfer and polishing method.

With SOI technology, there is concern that crystalline defects and lattice imperfections might cause various problems for high performance devices, by shortening the device life-time or reducing the efficiency of performance. In previous work, SOI-structures and have been characterised by Micro-beam Raman Spectroscopy[7], X-ray diffraction (XRD)[7]; cross-sectional high resolution transmission electron microscopy[8], white beam X-ray topography technique[9] and high-resolution nano-beam electron diffraction[10]. Here we report characterisation of SOI wafer structures by coherent X-ray diffractive imaging method, which produces real-space images of the defects with a resolution potentially reaching tens of nanometres.

1.3 Introduction to Coherent X-ray Diffractive Imaging

All the measurements reported here were performed at beamline 34-ID-C of the Advanced Photon Source at Argonne National Laboratory. Coherent X-ray Diffractive Imaging (CDI), especially using phase-contrast, is one of the strongest contenders for investigating internal structures (both atomic density and phases) of nanocrystalline materials [11-13]. More conventional imaging techniques such as Transmission Electron Microscopy (TEM) can only probe very thin cross-sections of the specimen under study. Any internal stresses could possibly be removed when samples are cross-sectioned to produce thin lamellar sections. On the contrary, with CDI, we can probe the 3-dimensional internal structure of entire samples without artificially damage samples.

The Coherent X-ray diffractive imaging technique has better reconstructed real-space resolution, presently around 30nm, than direct real-space imaging X-ray methods because of the inversion procedure used for the reciprocal-space diffraction patterns. This technique is able to investigate strains, seen as atomic displacements (from the ideal atomic position in a crystal lattice) of blocks of material with dimensions of 10nm to 1μm. It allows measurements of strains of individual regions while most diffraction techniques obtain results by averaging arrays of similar structures[14, 15].

2 Microbeam Methods and Results

2.1 Micro-beam Diffraction of SOI wafers

These measurements were performed by scanning a focussed 8.902keV X-ray beam across the sample while recording the diffraction pattern of an off-specular 111 reflection on a direct-detection CCD detector positioned 1.8m away from the sample. A grazing incidence angle of 5° was employed. The beam was focussed by Kirkpatrick-Baez (KB) mirrors to a probe size of about 1.5 microns and was made coherent by entrance slits of 10x20 microns placed before the mirrors. The beam was scanned along the direction parallel to the SOI surface and perpendicular to the beam direction (called "X" here) to study the variation of topography and mosaic structure of a typical SOI wafer.

Figure 1 shows key features extracted from the micro-diffraction measurements, after removal of positions which showed little variation. In many positions along the scan, there was just a single peak recorded, which varied in position on the detector, while in the positions highlighted there were two or even three peaks seen. The (x,y) position on the detector was converted into (roll,pitch) angular motions of the crystal lattice planes. The same scan performed on a standard Si(111) wafer showed no variation of peak positions, so the observed effect is not a property of the mechanical scanning stage (Newport model MFA) or other instrumentation. The typical distance in X-position from one-peak to two-peak of diffraction patterns or two- peak to three-peak is around 10 steps (5μm), which indicates that an average feature size is about 5μm. A similar scan along the Y-direction showed very little variation of diffraction patterns, presumably because the X-ray beam footprint along that direction is much longer, about 15 μm.

The results show strong variations of the centre of the rocking curves with splitting and de-splitting of peaks along this particular scanning path. The variations of positions of the peak maximum were due to surface topography or structure inhomogeneity of the SOI wafer, which might be a direct consequence of the film-transfer steps of the wafer fabrication procedure. Since it is possible the defects could affect the electrical properties of the material, it would be useful to apply this method as a routine diagnostic of the film transfer procedure.

Fig. 1 Micro-beam diffraction of of a typical SOI wafer. Upper panels: Roll(X direction) and Pitch(Y direction) orientations vs. position along X direction. The red, blue and black symbols represent the various positions of the peak maxima on the CCD . Some points where only a single peak was present have been removed. The pitch direction deviation is slightly bigger than that of the roll direction. The scan was performed with 5° of incidence angle, and 1800mm distance between the CCD detector and the specimen on the off-specular (111) reflection. Bottom panel: appearance on the CCD of micro-beam diffraction patterns at various X positions separated by around 9 microns. The intensity scales are the same for all patterns in the bottom panel.

2.2 Mosaic Structure and Split Diffraction Peaks

Splitting of peaks into two or three occurs when two distinct orientation are present in the sample at the same time. In a simple incoherent-beam model, the presence of two distinct peaks, rather than a smeared distribution, would mean that there is a sharp boundary between the grains, as in the classical picture of mosaicity. If clean fractures were present, passing right through the film, as suggested, this might have consequences for the electrical properties of the material. Mosaic structure in thin film single crystalline Silicon would be accompanied by dislocations or lattice faults between the crystal grains. In this model the peaks arise from the specific positions of the mosaic blocks within the whole structure; in this

case it is the summation of the diffracted intensities which can be very different for adjacent locations due to the variation the orientations of mosaic blocks. This would be expected to give abrupt jumps in otherwise straight lines tracking the peak positions, as illustrated by the solid lines in Figure 2.

In our experiment at APS, the beamline was designed to preserve the coherence of the X-rays. A coherent X-ray entering more than one mosaic block would result in interference patterns, resulting from linear superposition of the diffracted waves. This leads to an alternative explanation of the splitting of peaks because the contributions of neighbouring grains add coherently. Even if there are continuous variations of orientation between strained regions of single-crystalline structure, distinct peaks will arise because of the coherence. In a general way, the splitting of peaks can be modelled by a spatial variation of real-space phase, which can be linear ramps, parabolic or more complex phase variations[15]. An active field of research is looking into the kinds of phase structure that can explain complex mosaic structures by coherent X-ray diffraction [20].

The dashed lines in Fig 2 show schematically what we expect would happen under coherent X-ray illumination conditions. As interference effects turn on there would be a gradual shifting of the peaks, along with intensity variations. Even abrupt boundaries between undistorted mosaic blocks (as illustrated) would lead to smooth variations in peak position. In Fig 2 we see smooth evolution of the peak positions, but this does not allow us to tell whether the boundaries between mosaic regions of our SOI sample are abrupt or continuous. Further quantitative work should be able to answer this technologically important question.

Fig. 2 Illustration of the coherent and incoherent limits of diffraction from two overlapping mosaic grains. Upper panel: The black dotted line represents the edge of the object under study. The diagonal line represents a grain boundary separating two crystal mosaic blocks adjacent to each other. Lower panel: lines representing the positions of the peak maximum of diffraction patterns as a function of location of such a multi-grain crystal. The solid and dashed lines represent the expected variation in the fully incoherent and coherent limits respectively.

3 Bragg Coherent X-ray Diffractive Imaging

Beamline 34-ID-C at the Advanced Photon Source is dedicated to the coherent diffractive imaging technique, while it can also be used for the micro-beam experiment described above. 34-ID-C operates with horizontal and vertical KB mirrors, roller-blade slits, a Si(111) double-crystal monochromator and with an in-situ optical confocal microscope to pinpoint the exact locations of nanocrystals under study. The horizontal and vertical foci of our coherent X-ray beam were just under 1.6 and 1.7 µm respectively, and the energy used was 8.902keV for our experiment. Roller blades slits, before the KB mirror system, are used to define a coherent beam, which accept around 1% of the total flux of the incoming X-ray beam from the source.

The novelty of Coherent X-ray diffractive imaging lies in the fact that high coherence of the X-ray beam enables inversion of the diffraction patterns to three-dimensional (3D) images. The level of coherence enables us to obtain 3D diffraction patterns with high visibility of diffraction fringes that are the consequence of interferences between the coherently illuminated specimen edges in all three spatial dimensions. Measurements were taken in such a way that sufficient numbers of 2-dimensional frames with suitably small incremental steps

of rocking angle were obtained for successful reconstructions of real-space objects. An oversampling condition must be fulfilled so that the sampling frequency in reciprocal space is at least twice the bandwidth of the real space frequency. The measurements were taken in a mechanically stable environment, and the variations of humidity, temperature and other physical conditions were kept to a minimum. Figure 3 shows a 3D isosurface rendition of the measured diffraction pattern. There are strong fringes along the strong crystal truncation rod in the direction perpendicular to the wafer (approximate Qy direction) that arise from interference between the top and bottom surface of the SOI film.

Figure 3. Single 3D isosurface of the measured diffraction pattern of a coherent X-ray beam penetrating through a SOI unpatterned wafer. The theta rocking curve step size is 0.001 degree with 100 frames. The distance between the detector and the specimen is 1800mm. The angle of incidence of X-ray beam is 13º at the off-specular (111) Bragg reflection.. The indicated Qx and Qy are in the approximate horizontal and vertical directions across the beam. Raw pixel coordinates have been used, so the scale is not authentic. The sample is lying horizontally (at incidence angle of 13º) with the incident beam along the z-direction.

By studying a commercial SOI wafer, we were able to look directly at the coherent X-ray beam profile by inverting this diffraction pattern, generated by the coherent X-ray beam directly penetrating the thin crystalline film specimen. We successfully obtained density profile reconstructions with the previously developed Error-Reduction (ER) and Hybrid-Input-Output (HIO) iterative algorithms[13]. In fig 4, these images of the beam intersecting the SOI film are compared with the dimensions and orientation expected for the beam's 13º angle of incidence used in the experimental measurements. The Fourier transform of our experimental image result and the actual X-ray diffraction measurements are in excellent agreement with each other.

Fig. 4 Top: Schematic diagram of the incident coherent X-ray beam diffraction geometry on the SOI sample at 13º angle of incidence with the beam propagation direction marked with arrows. Middle: Single isosurface of reconstructed three-dimensional amplitude of beam profile within the SOI film. Bottom: the corresponding scalar-cut-plane through the as-determined density profile of the X-ray beam illumination.

The top and bottom surfaces of the 3-dimensional reconstructed amplitude appear flat, well-defined and separated by about the right distance, 650nm. This agrees with the measured specification from the manufacturer of the Silicon layer of our SOI sample (600nm ± 100nm). However, the sides of the reconstructed amplitude appear rough, wavy and are much less defined comparing with the top and the bottom surfaces. This waviness could be explained by the lack of interference fringes in the Qx and Qz directions of the data. The incident coherent X-ray beam was under 2µm for both directions and this is seen in the image. The approximately Gaussian profile of the beam in the Qx and Qz directions appears in the Fourier transform as a Gaussian image (with noise) in the x-z cross-sectional plane.

The angle of incidence was measured to be around 13º± 3º in the reconstructed image in figure 4, shown at isosurface level of 0.164 of the maximum contour of the reconstructed amplitude using Mayavi visualiser version 1.5. The dimensions of the reconstructed amplitude are 1.3±0.13, 0.65±0.065 and 3±0.3 µm for the x, y and z directions respectively. These are within reasonable range of the actual experimental setup parameters and SOI wafer dimensions. The beam width in the x direction, measured to be around 1.3±0.13 µm in the reconstructed image, is slightly smaller than the horizontal focus size, as measured by

scanning a Tungsten wire. The discrepancy is possibly due to absorption of X-ray beam by the wire and scattering effect of the beam by the wire.

The interference of the coherent X-ray beam diffracting from the SOI surface structure layer in Fig 3 shows fringes with less visibility than expected for a fully coherent beam. Because the entrance slits were considerably smaller than the expected coherence lengths in the horizontal and vertical, we do not think this is a transverse coherence effect. The reduced visibility of the fringes could be attributable to the limited longitudinal coherence of the beam[16]. This leads to partial breaking of the conditions for oversampling to work, which might cause the borders of the resulting image to be less well-defined consequently. Corrections of the phasing algorithms for partial coherence effects are another future direction of this research.

4 Discussion and Future Outlook

Our results open an interesting and useful horizon for direct imaging and understanding of technological materials. We are interested in how a coherent X-ray beam of synchrotron radiation interacts with samples under various experimental conditions and how these interactions can be interpreted in terms of physical properties of the sample.

Recent development of Strained Silicon-On-Insulator (SSOI) has brought enormous attention to this as a new industrial material. Systematic studies of SSOI structures by X-ray topography, Raman scattering, atomic force microscopy and cross-sectional high-resolution TEM[17, 18] have been carried out, and most of the references indicate that the strain generated by lattice mismatches between SiGe and Silicon layer is not affected by further processing such as transferring or annealing of thin silicon film[2, 19]. Coherent X-ray diffractive imaging studies on SSOI samples are planned in the near future to obtain a better understanding of the distribution and evolution of strains caused by lattice mismatches between crystals and the causal stresses or pressure. Furthermore, investigation of strain evolution during industrial processing is particularly important for comprehension of silicon-based devices performance and the corresponding strain-associated causes of device failure.

Our micro-beam diffraction experiments strongly indicate that structural inhomogeneities were present in the Silicon-On-Insulator unpatterned continuous wafer we investigated. The results were analysed and the peak-splitting in diffraction patterns measured is most likely the consequences of mosaic crystal structure, which might indicate that there are grains within a single SOI wafer are separated by grain boundaries. Further studies are needed for thorough understanding of possible distribution and evolution of strain in these thin Silicon layers under various physical conditions.

Acknowledgements

The experimental work was carried out at APS beamline 34-ID-C, built with funds from the US National Science Foundation under grant DMR-9724294 and operated by the U.S. Department of Energy, Office of Science, Office of Basic Energy Sciences, under Contract No. DE-AC02-06CH11357. The research was supported by the European Rerearch Council “Advanced” grant “Nanosculpture” code 227711

References and Notes

1. Henry, M.D., et al., *Ga+beam lithography for nanoscale silicon reactive ion etching.* Nanotechnology, 2010. **21**(24): p. 245303.
2. Drake, T.S., M.L. Lee, A.J. Pitera,. E.A. Fitzgerald, D.H. Anjum, J. Li,, N.K. R. Hull, and J.L. Hoyt, *Fabrication of Ultra-Thin Strained Silicon on Insulator.* Journal of Electronic Materials, 2003. **32**(9): p. 972-975.
3. Jaju, V., *Silicon-On-Insulator Technology*, in *Advances in MOSFETs EE530*. 2004.
4. U.S. Patent 5,061,642 Method of manufacturing semiconductor on insulator, Hiroshi Fujioka, Issue date: Oct 29, 1991
5. Bich-Yen Nguyen, G.C., and Carlos Mazuré, A *Review of SOI Technology and its Applications.* Journal Integrated Circuits and Systems, 2009. 4(**2**): p. 51-54.
6. B. Aspar, M.B., H. Moriceau, C. Maleville, T. Poumeyrol, A.M. Papon, B*asic mechanisms involved in the Smart-Cut process.* Microelectronic Engineering, 1997. 36(**1**-4): p. 233-240.
7. Paillard and V., *Strain characterization of strained silicon on insulator wafers.* Microelectronic Engineering, 2004. 72(**1**-4): p. 367-373.
8. Moutanabbir, O., et al., N*anoscale patterning induced strain redistribution in ultrathin strained Si layers on oxide*. Nanotechnology, 2010. 21(**1**3): p. 134013.
9. Fukuda, K., et al., Wh*ite X-ray Topography of Lattice Undulation in Bonded Silicon-on-Insulator Wafers.* Japanese Journal of Applied Physics, 2006. 45(**N**o. 9A): p. 6795-6799.
10. Usuda, K., et al., *Strain characterization in SOI and strained-Si on SGOI MOSFET channel using nano-beam electron diffraction (NBD).* Materials Science and Engineering: B, 2005. 12**4-125:** p. 143-147.
11. Marcus C. Newton1, S.J.L., Ross Harder and Ian K. Robinson, Thr*ee-dimensional imaging of strain in a single ZnO nanorod.* Nature Materials, 2010. 9: p. 120-124.
12. Harder, R., et al., Im*aging of complex density in silver nanocubes by coherent x-ray diffraction.* New Journal of Physics, 2010. 12(**3**): p. 035019.
13. Robinson, I. and R. Harder, C*oherent X-ray diffraction imaging of strain at the nanoscale.* Nature Materials, 2009. 8(**4**): p. 291-298.
14. Divine P. Kumah, S.S., Yossi Paltiel, Yizhak Yacoby and Roy Clarke, At*omic-scale mapping of quantum dots formed by droplet epitaxy.* Nature Nanotechnology, 2009. 4: p. 835-838.
15. A. A. Minkevich, E.F., T. Slobodskyy, M. Riotte, D. Grigoriev, and A.C.I. M. Schmidbauer, V. Nov´ak, V. Hol´y, and T. Baumbach, S*elective coherent x-ray diffractive imaging of displacement fields in (Ga,Mn)As/GaAs periodical wires.* Materials Science (cond-mat.mtrl-sci), 2009. ar**Xiv:0909.4711v1 [cond-mat.mtrl-sci].**
16. Steven J. Leake, M.C.N., Ross Harder, and Ian K. Robinson, Longitudinal Coherence Function in X-ray Imaging of Crystals Optics Express, 2009. 17(**1**8): p. 15853-15859.
17. Black, D.R., et al., Im*aging defects in strained-silicon thin films by glancing-incidence x-ray topography.* Applied Physics Letters, 2006. 88(**2**2): p. 224102.
18. Langdo, T.A., et al., Si*Ge-free strained Si on insulator by wafer bonding and layer transfer.* Applied Physics Letters, 2003. 82(**2**4): p. 4256.
19. Erdtmann, M. and T.A. Langdo, The *Crystallographic Properties of Strained Silicon Measured by X-Ray Diffraction.* Journal of Materials Science: Materials in Electronics, 2006. 17(**2**): p. 137-147.

20. Aranda, M. A. G., F. Berenguer, R. J. Bean, Xiaowen Shi, Gang Xiong, S. P. Collins, C. Nave and I. K. Robinson, Coherent X-ray diffraction characterization of twinned microcrystals, accepted in Journal of Synchrotron Radiation (2010)

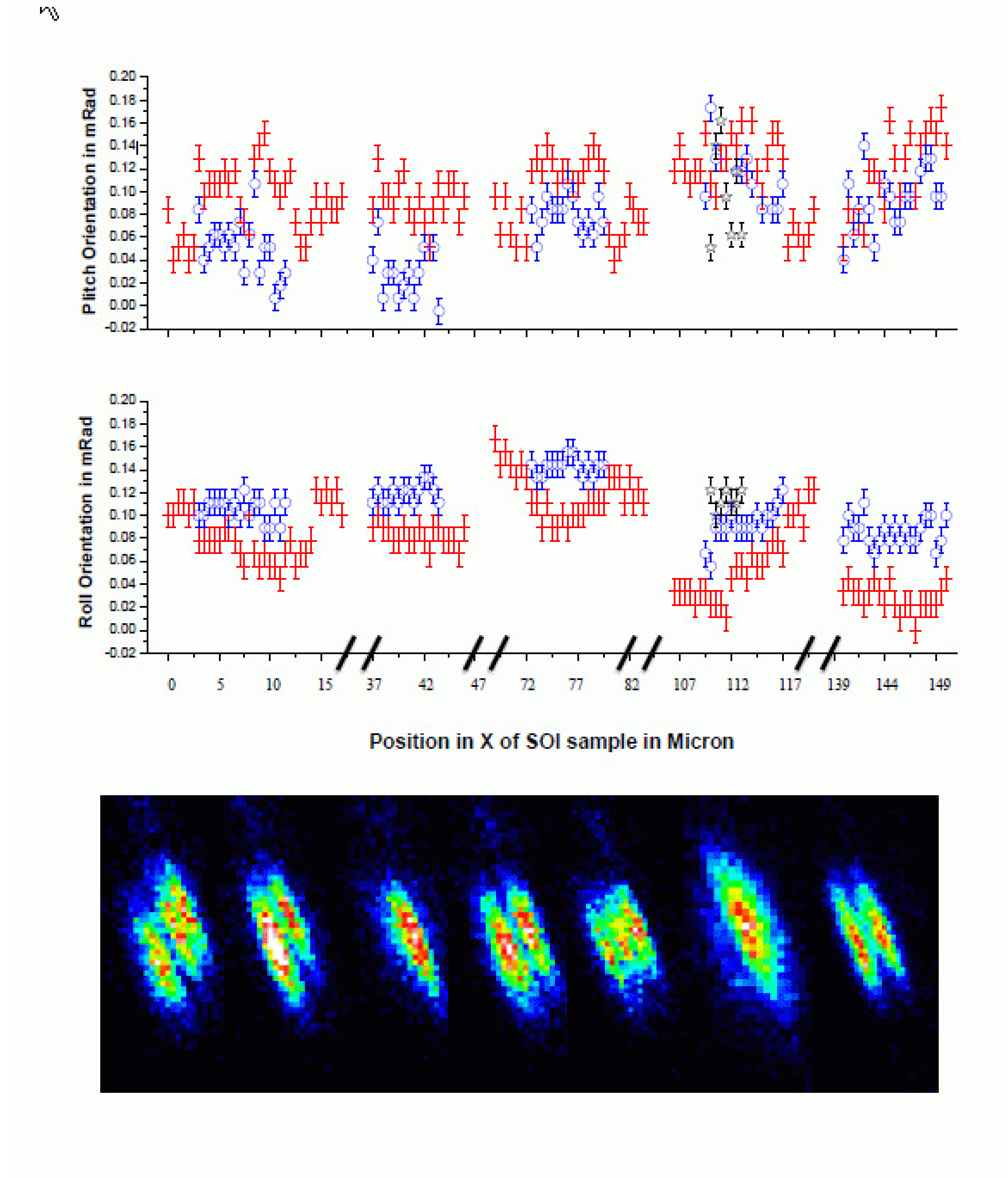

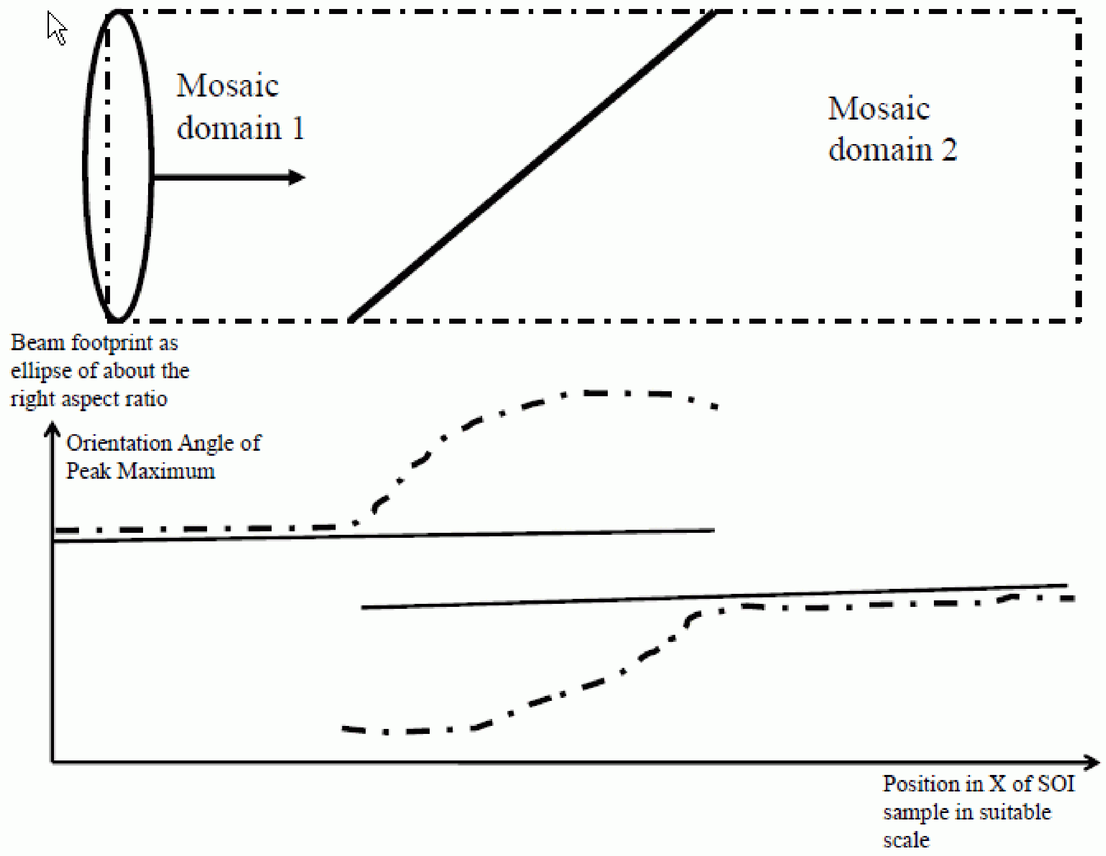
Mosaic
domain 1
Mosaic
domain 2
Beam footprint as
ellipse of about the
right aspect ratio
Orientation Angle of
Peak Maximum
Position in X of SOI
sample in suitable
scale

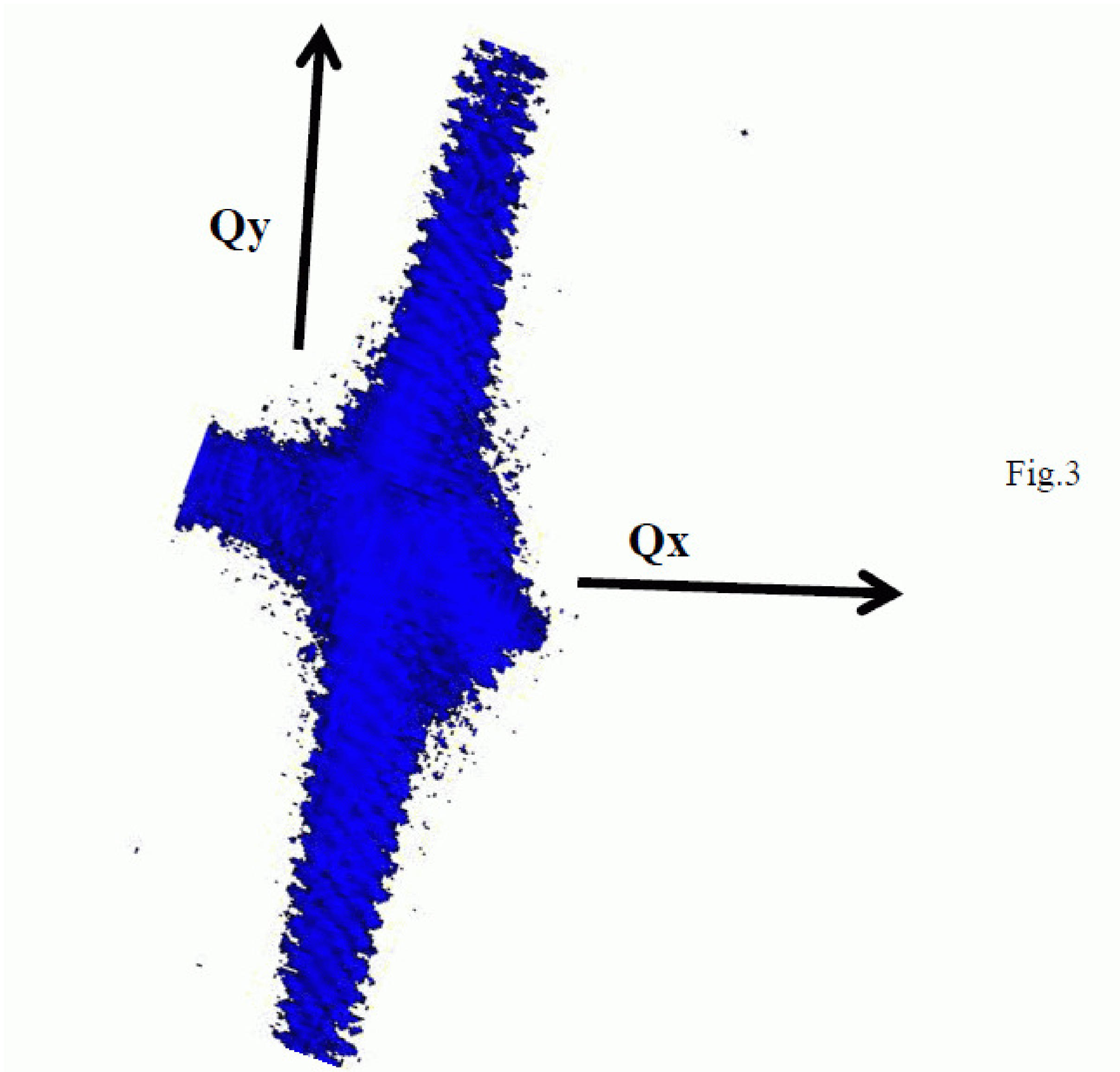

Fig.3

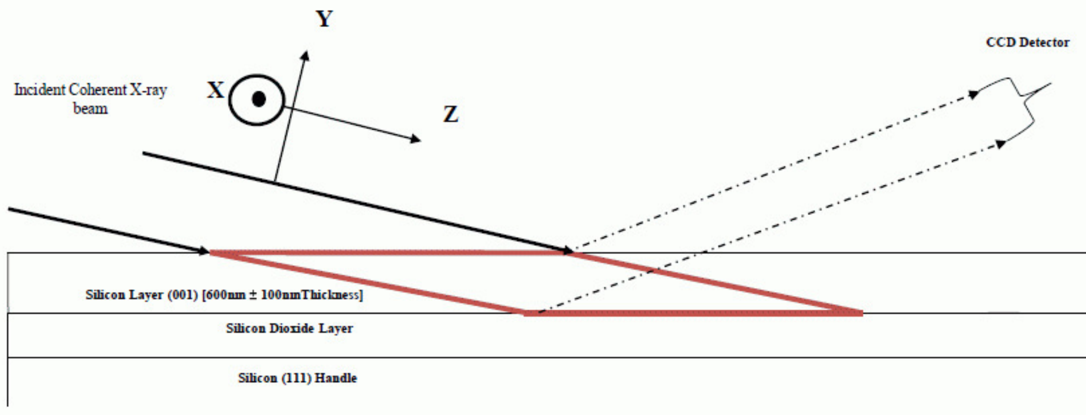
Y
CCD Detector
Incident Coherent X-ray beam
X
Z
Silicon Layer (001) [600nm ± 100nmThickness]
Silicon Dioxide Layer
Silicon (111) Handle

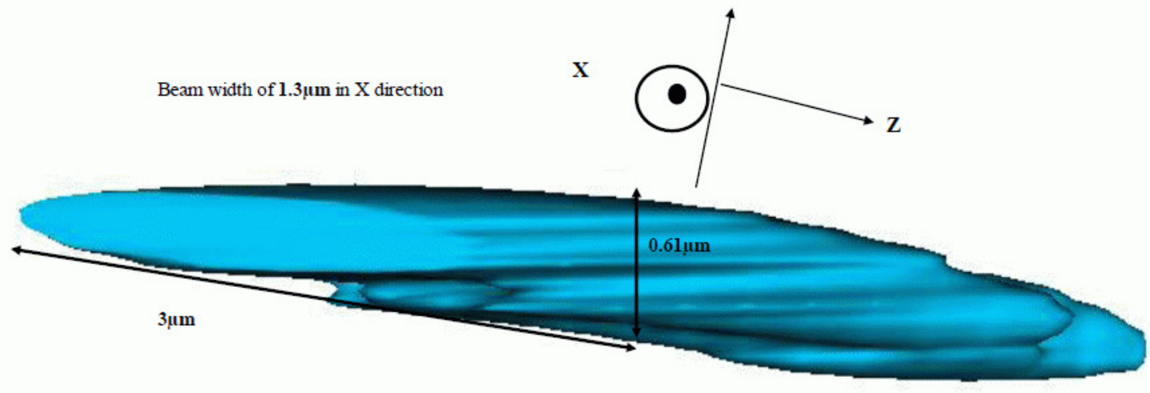
Beam width of 1.3μm in X direction
X
Z
0.61μm
3μm